DOI: 10.1007/s12541-010-0088-y

Surface Texturing by Micro ECM for Friction Reduction

Jung Won Byun[1], Hong Shik Shin[1], Min Ho Kwon[1], Bo Hyun Kim[2,#] and Chong Nam Chu[1]

1 School of Mechanical and Aerospace Engineering, Seoul National University, 599 Gwanak-ro, Gwanak-gu, Seoul, South Korea, 151-742
2 Department of Mechanical Engineering, Soongsil University, 511 Sangdo-dong, Dongjak-gu, Seoul, South Korea, 156-743
Corresponding Author / E-mail: bhkim@ssu.ac.kr, TEL: +82-2-820-0653, FAX: +82-2-820-0668

KEYWORDS: Surface texturing, Friction reduction, Micro ECM, Micro dimple

Surface texturing with micro-dimples is a known method for friction reduction under lubricated sliding contact, and various machining techniques have been researched and developed in order to fabricate micro-dimple patterns. However, previous fabrication methods possess several problems, such as causing thermal damage on the workpiece or limiting the available workpiece geometry. In micro ECM, micro features can be machined without any resulting thermal or mechanical damage. From this perspective, micro ECM has certain advantages over surface texturing. Also, micro ECM is applicable to non-planar workpieces. In this research study, micro ECM with microsecond pulses was applied in order to fabricate a micro-dimple pattern. The machining characteristics were investigated in fabricating micro dimples on AISI 440C specimen. On the basis of the experimental results, a Ø 300 μm dimple pattern was successively produced on the AISI 440C specimen. A friction test on the textured specimen was performed and compared with a non-textured specimen. The enhancement of frictional performance was successfully demonstrated experimentally.

Manuscript received: April 8, 2010 / Accepted: June 10, 2010

NOMENCLATURE

c = double layer capacitance
R_s = electrolyte resistance
τ = charging time constant
ρ = specific resistivity
d = distance between electrodes
ϕ_c = charged potential of the double layer
ϕ_0 = applied potential
t_p = pulse on-time

1. Introduction

Reducing friction is necessary in order to save energy and improve the wear properties of mechanical components. For decades, surface topography and texture design have been researched to enhance the tribological properties of frictional surfaces. One example of such research involved the introduction of patterning using micro dimples by several research groups worldwide.[1] It was reported that micro-dimpled patterns fabricated at a shallow depth played a useful role in creating micro hydrodynamic bearings and retained the lubrication film.[2,3] Hydrodynamic pressure is built up in a dimple on the sliding surface. With this generated pressure, a thicker film forms in the dimpled surface than on the flat surface. The load on the contact is actually supported by the fluid film, and a thick fluid film prevents solid-solid contact between the sliding surfaces. As a result, friction reduces, compared with flat surfaces, and the machine operates more effectively and with less wear and tear.

Several fabrication techniques, such as chemical etching, abrasive jet machining, reactive ion etching, and laser machining have been utilized to produce micro-dimple patterns on surfaces.[4-13] However, there are some limitations in these techniques when they have been employed in practical efforts. For example, photolithographic processes are used in chemical etching, abrasive jet machining, and reactive ion etching. However, these kinds of methods are carried out through complicated processes, and it is hard to fabricate patterns on the non-flat surfaces using this technology. Nanosecond lasers have been used for surface texturing and can produce micro patterns swiftly.[8] However, nanosecond laser machining of metals may generate heat affected zone.[9]

For surface texturing of metals, electrochemical machining (ECM) also has been used. In micro ECM, micro-sized features can

be machined by using short voltage pulses.[14,15] However, machining conditions including electrolyte and pulse should be selected carefully to improve machining resolution. Micro ECM is much slower than other techniques. To increase productivity, usage of batch tools was introduced.[16] ECM does not produce mechanical or thermal damage, burrs, and debris because metal is electrochemically dissolved. In contrast to chemical etching using mask, micro ECM is a maskless process. Therefore, it can generate textures not only on planar surface but non-planar surface where mask is not easy to fabricate.

In this paper, micro ECM, which uses short pulses of a microsecond pulse on-time, was applied to fabricating micro-dimple patterns and machining conditions for desired dimple dimensions were investigated. As a result, the surface texture with micro dimples was successfully machined on planar or non-planar specimens. A friction test was performed on the patterned specimen and the results showed an enhancement in the overall frictional performance compared with the flat specimen.

2. Experimental Setup

2.1 Workpiece material and electrolyte

AISI 440C is a type of modern carbon steel famous for its wear resistance, strength, and hardness. Since it is capable of attaining high hardness after heat treatment and allows creation of a smooth polished surface, AISI 440C has been widely used for sliding components. In this research, AISI 440C hardened by heat treatment was used as a workpiece for surface texturing.

Acidic electrolytes have been used to fabricate micro-features on passivating metals in ECM.[14,16-20] This is because zero sludge formation is advantageous for accurate machining. However, AISI 440C, a kind of carbon steel, is corrosive in acidic solutions. To prevent corrosion of the substrate, sodium nitrate, a kind of neutral solution, was used as an electrolyte in this research.

2.2 System

Fig. 1 shows the experimental system for micro ECM. A tool electrode and a workpiece were mounted to a three-axis positioning stage, and polished AISI 440C served as the workpiece. A tool electrode of brass was machined into a cylinder shape of Ø 250 μm using a wire EDM. To minimize stray current, the sidewall of the tool electrode was insulated with diluted enamel. The electrochemical cell consisted of a workpiece, a tool electrode, an electrolyte, a counter electrode (CE), and a reference electrode (RE). The RE and CE were platinum wires, and the electrolyte used was 2 M sodium nitrate. A pulse generator was used to produce pulses of a few microseconds, applying the voltage between the tool electrode and the workpiece. During the pulse off-time, the potentials of the tool electrode and the workpiece should be maintained at chemically stable regions to prevent undesirable chemical reaction; in this case, a potentiostat controlled the potential of the workpiece via the CE and the RE. The potential of the tool electrode was adjusted using the offset voltage of the pulse generator as shown in fig. 2. To minimize the effect of impedance, a voltage follower was connected between the pulse generator and the tool electrode.

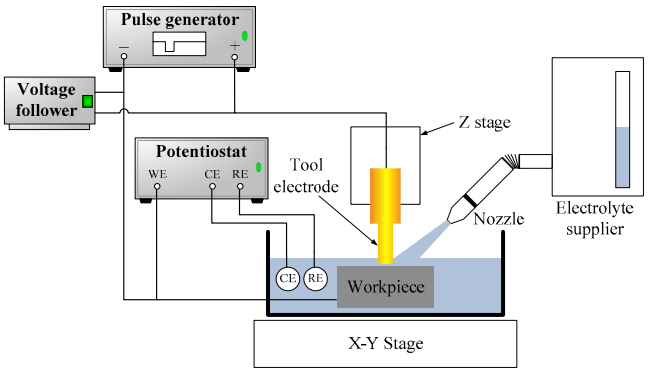

Fig. 1 Schematic diagram of the electrochemical machining system

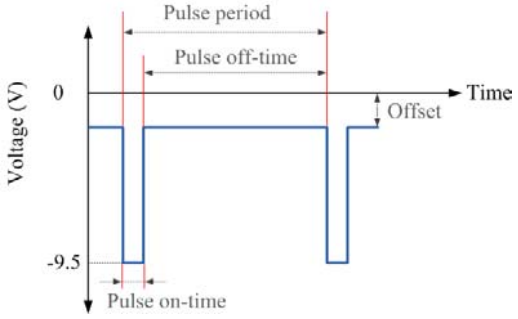

Fig. 2 Pulse shape applied on the tool electrode

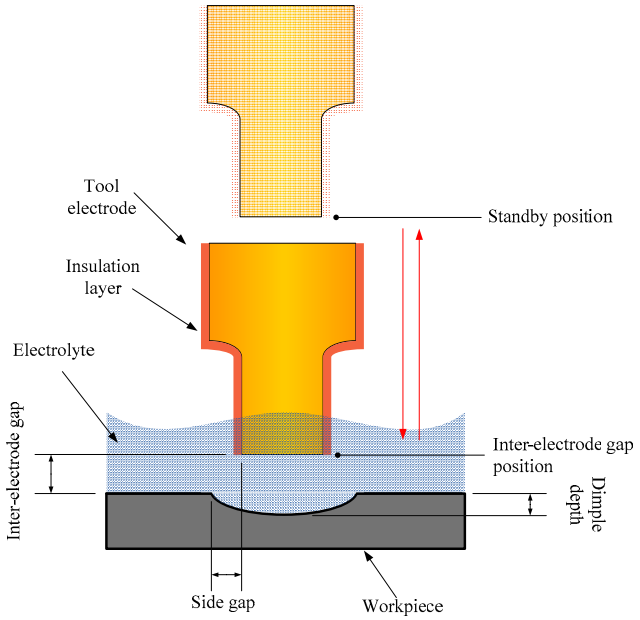

Fig. 3 Detailed view of the tool electrode and the workpiece during ECM

The electrochemical reactions that took place during ECM in the sodium nitrate electrolyte are set forth below:

$$\text{Anodic reaction: } Fe + 2(OH)^- \rightarrow Fe(OH)_2 + 2e^- \quad (1)$$

$$\text{Cathodic reaction: } 2H_2O + 2e^- \rightarrow H_2 + 2(OH)^- \quad (2)$$

Since sludge of metal hydroxide is produced on the workpiece

during ECM in the sodium nitrate electrolyte, the electrolyte was supplied to the electrochemical cell equipped with injection to flush away produced sludge. To duplicate the shape of the tool electrode onto the workpiece to a high degree of accuracy, machining should be carried out with a very narrow inter-electrode gap, which may cause local shortage of ions or accumulation of sludge. To prevent these phenomena, machining was performed in a pecking manner: the tool electrode moved down from a height of standby position to the inter-electrode gap position, and after 1 s of dwell time, it returned to the standby position rapidly. This cycle repeated several times for each dimple machining. Fig. 3 illustrates pecking machining procedure.

3. Determination of electrochemical machining conditions

The lubrication performance of the textured surface varies with the dimensions of the micro-dimpled pattern. Relevant factors to be taken into account include: the dimple diameter, depth, and areal density. In results obtained by Wang, *et al.*, the textured surfaces with dimple diameters in the range of 300 to 400 μm showed good lubrication performance in conformal contacting conditions.[21] In these dimple sizes, the proper depth of each dimple was about 5~10 μm, and the areal density was between 5 and 10%. The depth of the dimples should be continuously well-controlled because deep dimples are not beneficial for lubrication.[3,22]

In order to achieve a shallow machining depth of the dimples, machining characteristics according to electrode potentials, pulse conditions, and machining time were investigated. With these conditions, a side gap of dimple varied. Since the shape of an electrode is transferred to the workpiece, the electrode diameter can be estimated by taking into consideration the side gap.

3.1 Determination of electrode potential

An inappropriate potential can cause unfavorable electrochemical reactions. Corrosion or dissolution of electrodes may occur without the potential control of electrodes. If overall corrosion occurs on electrodes, surface integrity, such as roughness, may be worsened. Also, dissolution of the tool electrode due to inappropriate potential may cause distortion of machined features, because tool shape and inter-electrode gap may change during machining.

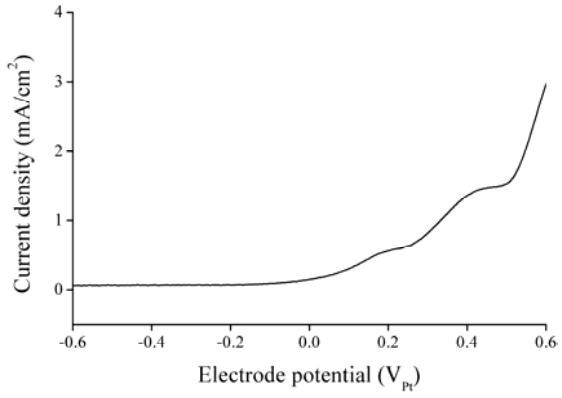

Fig. 4 Polarization curve of AISI 440C (RE: Pt, CE: Pt, electrolyte: 2M $NaNO_3$)

To investigate electrochemical behavior with potential, linear sweep voltammetries of the workpiece and the tool electrode were performed in 2 M sodium nitrate solution. Fig. 4 shows the polarization curve of AISI 440C. The reaction current was measured according to the potential at a scan rate of 10 mVs^{-1}. Since the current begins to increase near -0.2 V_{pt}, the workpiece potential should be placed under -0.2 V_{pt} in order to prevent its overall dissolution. However, when the workpiece potential was set to -0.3 ~ -0.2 V_{pt}, pitting was found around the machined dimple, as shown in fig. 5(a). It can be supposed then that the passive film around the machined dimple was weakened during machining and could not protect the workpiece from corrosion. When the workpiece potential was set to -0.5 ~ -0.4 V_{pt}, pitting around the dimple could be prevented, as shown in fig. 5(b).

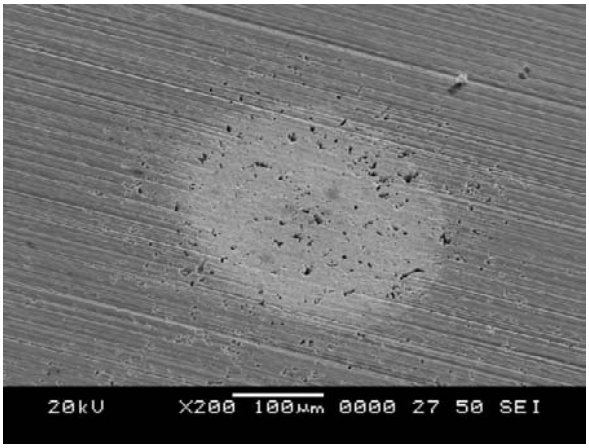

(a)

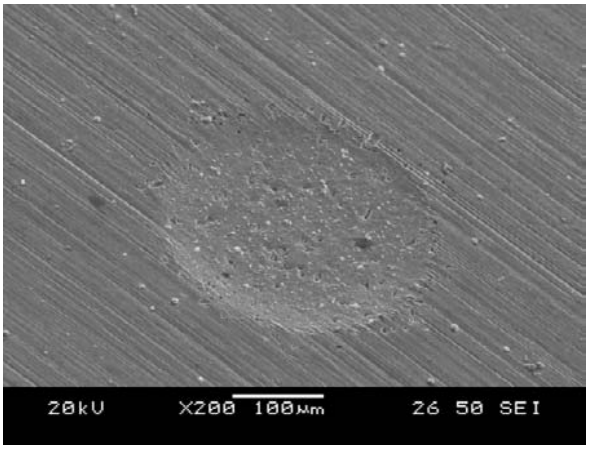

(b)

Fig. 5(a) Machined dimple at -0.2 V_{pt} workpiece potential (pulse: 9.5 V, 2 μs/20 μs, inter-electrode gap: 30 μm, pecking repetition: 10), (b) Machined dimple at -0.4 V_{pt} workpiece potential (pulse: 9.5 V, 2 μs/20 μs, inter-electrode gap: 30 μm, pecking repetition: 10)

Like the workpiece electrode, the surface of the tool electrode is affected by its potential. In fig. 6, the passive region of the brass ranged from -0.8 V_{pt} to -0.7 V_{pt} and the current increases at -0.7 V_{pt}. Therefore, the potential should be less than -0.7 V_{pt} so as not to

dissolve the entire electrode. Hence, the potential of the tool electrode was placed in the electrochemically stable region of from -0.8 to -0.7 V_{pt}.

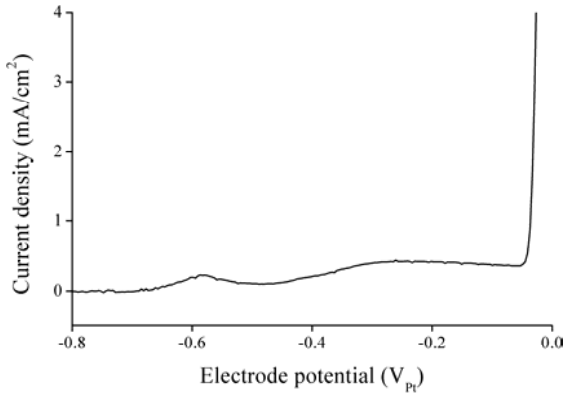

Fig. 6 Polarization curve of brass (RE: Pt, CE: Pt, electrolyte: 2 M $NaNO_3$)

3.2 Machining gap variation with pulse on-time and machining time

The electrochemical cell, which consists of the tool electrode and the workpiece in the electrolyte, can be considered to be an electric circuit. As shown in fig. 7, it can be expressed as the equivalent RC circuit that consists of capacitors and resistors, where electrolyte resistance (R_s) is the product of the specific resistivity (ρ) and the distance (d) between the electrode and the workpiece. The charging time constant (τ) for a double layer is:[15]

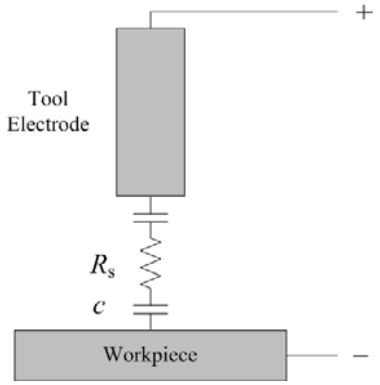

Fig. 7 The electrical double layer model[15]

$$\tau = \rho c d \tag{3}$$

where c is the specific capacitance of the double layer.

When short pulses are applied between electrodes, the maximum charged potential of the double layer according to the distance (d) is:[20]

$$\phi_c(t) = \frac{\phi_0}{2}\left[1 - \exp\left(\frac{t_p}{\tau}\right)\right] = \frac{\phi_0}{2}\left[1 - \exp\left(\frac{t_p}{\rho c d}\right)\right] \tag{4}$$

where ϕ_0 is the on-time voltage, t_p is the pulse on-time.

From equation (4), the workpiece will only be charged where the local τ does not considerably exceed the pulse on-time (t_p). In the fixed inter-electrode gap condition, the level of localization of reaction can be determined by the pulse on-time. Therefore, a machining gap can be controlled by changing the pulse on-time.

Another parameter to determine the dimension of the machined feature is machining time. In the pecking machining, anodic dissolution only takes place at the inter-electrode gap position during 1 s of dwell time. Hence, the pecking repetition number means machining time. In order to investigate variations in dimple dimensions according to pulse on-time and pecking repetition number, experiments on single dimple machining were performed.

The inter-electrode gap was maintained at 30 μm. In the ECM process, smaller inter-electrode gap enables more accurate transfer of a tool electrode theoretically. However, in experimental conditions under 30 μm of inter-electrode gap, anodic dissolution was restricted because a hydrogen bubble generated on the tool electrode was trapped between the narrow gap instead of being ejected.

When the pulse on-time condition was shorter than 1 μs, anodic dissolution hardly occurred. This is because the potential of the double layer cannot be sufficiently charged at 30 μm spacing in the very short pulse on-time. In order to fabricate dimples with sufficient depth, the pulse on-time condition should be set to longer values of over 1 μs. Hence, the experimental condition for the pulse on-time started from 2 μs to 22 μs. At each pulse on-time condition, experiments were performed with pecking repetition of 5, 10, 15, 20, and 25 times. In all experimental conditions, the duty ratio (i.e., pulse on-time:pulse period) was set to 1:10. An on-time voltage of 9.5 V was applied to the electrochemical cell using the pulse generator.

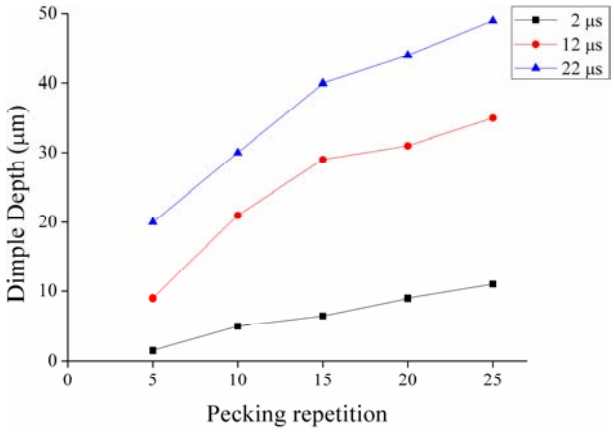

Fig. 8 Dimple depth according to the pulse on-time and the machining time

Fig. 8 shows the dimple depth variations according to pulse on-time and pecking repetition. In all conditions of pulse on-time, dimple depths increased as the machining time increased. When a pulse on-time of 2 μs was applied, the dimple depth slightly increased with an increase in the machining time. However, in a pulse on-time of 12 and 22 μs, rapid increases in depth were found in pecking repetition number. The dimple depth under 10 μm can be achieved at the condition of 12 μs pulse on-time with a repetition number of 5. However, side gap was larger than in 2 μs pulse on-time, as shown in fig. 9. To fabricate a shallow dimple of about 5

μm with high accuracy, a 2 μs pulse on-time with 10 times pecking repetition is appropriate.

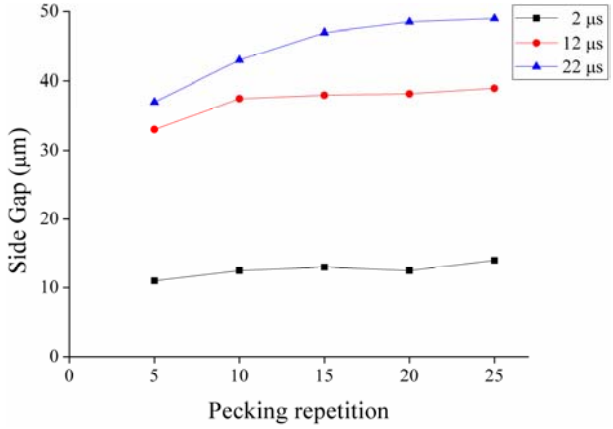

Fig. 9 Side gap according to the pulse on-time and the machining time

The dimple diameter can be predicted by the addition of electrode diameter and side gaps. Since the side gap was about 12 μm in 2 μs pulse on-time and 10 times pecking repetition, the diameter of a tool electrode was set to 275 μm in order to fabricate dimples with a diameter of 300 μm.

4. Fabrication of surface textures

4.1 Surface texture patterning

Before micro ECM surface texturing, a workpiece of AISI 440C was machined to a pin shape of which the top was polished. It was designed to be utilized for a friction test and, after installation in the electrochemical bath, the alignment between the top surface of the workpiece and the axis of the stage was adjusted.

For the texture pattern on the workpiece, the position set of the dimples was programmed into a motor controller. The distance between the dimples was 1 mm and the total dimple number was 37, which means 5 % of areal ratio.

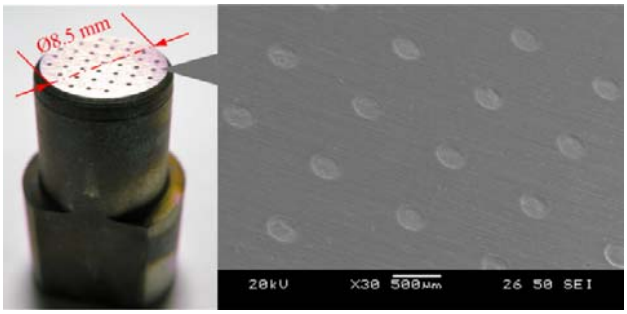

Fig. 10 Surface textured specimen and SEM of dimpled pattern

Fig. 10 shows a scanning electron microscope image of the patterned surface. The diameter of each dimple was about 300 μm. The dimpled surface was measured by the surface profiler. Fig. 11 shows the profile of dimples along the scanning direction. Shallow dimples of about 5 μm in depth were well defined repeatedly.

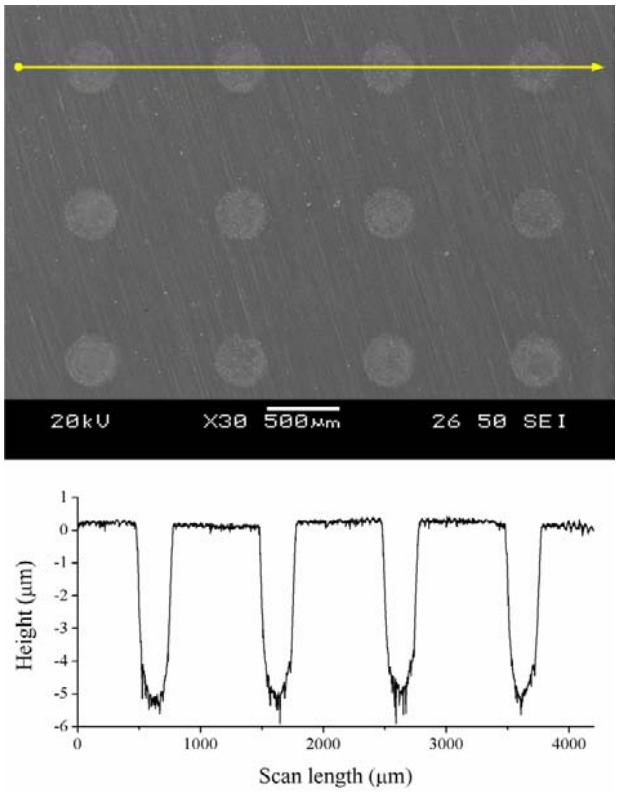

Fig. 11 The arrangement of micro dimples and cross section profile

4.2 Surface texture patterning on the non-planar surface

To machine a dimple pattern on a non-planar surface, the geometry of a workpiece should be taken into account. To fabricate a dimple pattern on the step-shaped surface, the trajectory of the electrode was programmed according to the geometry of the workpiece. The result of surface texturing is shown in fig. 12.

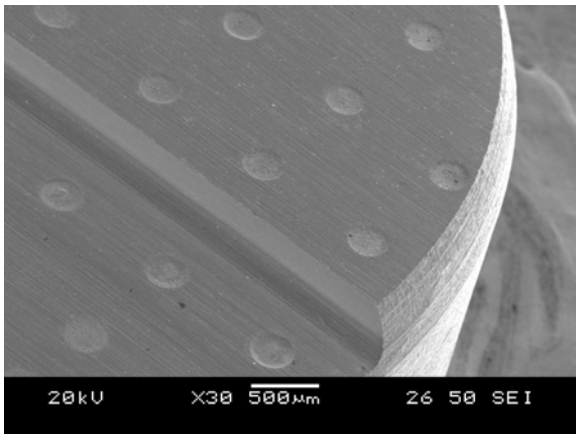

Fig. 12 Dimple pattern on the step-shaped specimen

5. Friction test

5.1 Experimental details

To evaluate the lubrication performance of the patterned surface, a friction test was performed using a pin-on-block tribometer. Fig. 13 shows the constitution of the tribometer. A textured or flat pin was assembled to the pin holder. The pin holder was designed with

a ball joint in order to maintain conformal contact between the pin and counter surface. A normal load was imposed using weights, and a reciprocating motion was produced by the linear moving stage at various sliding speeds. During the friction test, the friction force was measured by a dynamometer. Commercial lubricant oil (Shell helix) was used for this study. The physical properties of the lubricant are presented in table 1.

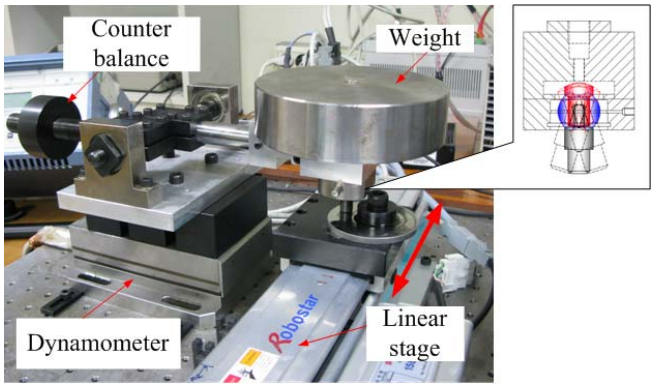

Fig. 13 Constitution of the tribometer

Table 1 Physical properties of lubricant oil used for test

Kinematic viscosity (cSt) at		Pour point (°C)	Flash point(°C)
40 °C	100 °C		
57.0	10.1	-36	220

The friction test was conducted at a normal load of 150N, corresponding to a normal contact pressure (load/nominal contact area) of 2.98 MPa. The test was performed at sliding speeds of 10, 12.5, 15, 17.5, 20, 25, 30, 40, 60, and 80 mm/s. At each sliding speed condition, the friction force was measured by the dynamometer at the sampling rate of 500 sample s^{-1}. The friction force data were averaged and converted to a friction coefficient (friction force/normal load).

5.2 Effect of dimple texture on friction coefficient

Fig. 14 shows the friction variations of the flat and textured surfaces. The results for the textured surface indicate a significant drop in the friction coefficient, especially at low-speed conditions. The results indicate that a lubricant film was formed more effectively on the textured surface compared with the flat surface. At higher sliding speeds, the differences in the friction coefficients between the two surfaces became smaller, because both contacts reached the full film lubrication regime. These results confirm and support the view that micro-dimples promote the formation of lubricants, resulting in the reduction of levels of friction.

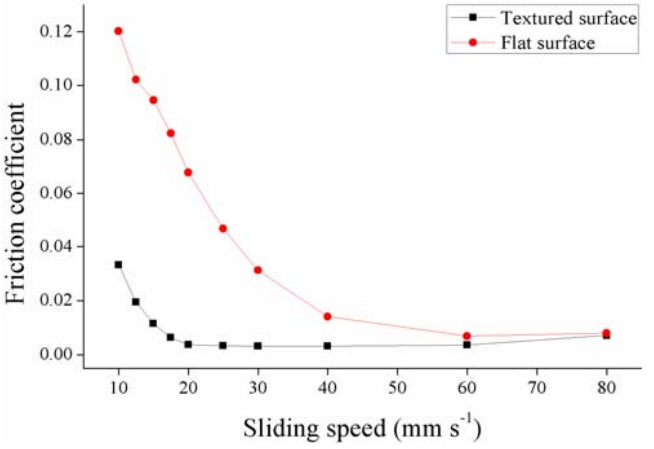

Fig. 14 Variation of the friction coefficient with sliding speed

6. Conclusion

This paper has suggested micro ECM as a new surface texturing method. With this method, neither thermal nor mechanical damage remain after pattern machining. Also, this machining process is simple when compared to photolithographic processes. Since deep dimples have a negative effect on frictional performance under a lubricated sliding contact, the dimensions of the dimples should be carefully controlled. For the stable fabrication of shallow dimples, machining conditions in micro ECM were investigated. Results showed that the depth of the dimples can be controlled by varying the pulse on-time and machining time. Dimples of about 5 μm in depth were successfully machined under conditions of a 2 μs pulse on-time and 10 s of nominal machining time. The diameter of the dimple can be determined by the tool diameter, while considering the side gap. With a Ø 275 μm tool electrode, dimples of 300 μm in diameter and 5 μm in depth were successfully fabricated on the workpiece. During dimple machining, the electrode potentials were controlled by the potentiostat and the offset of the pulse generator, as undesired electrochemical reactions on the electrodes may occur without potential control. As a result, it was possible to fabricate patterns with shallow dimples on the AISI 440C specimen. Additionally, the fabrication of surface texture on the non-flat surface was made possible by ensuring the adequate trajectory of the tool electrode.

To investigate the frictional characteristics of the textured surface, a friction test was performed and compared with the properties of the flat surface. A considerable improvement in the friction coefficient was achieved for the textured surfaces.

ACKNOWLEDGEMENT

This work was supported by the Korea Science and Engineering Foundation (KOSEF) grant funded by the Korea government (MEST) (No. 2010-0000441).

REFERENCES

1. Bruzzone, A. A. G., Costa, H. L., Lonardo, P. M. and Lucca, D. A., “Advances in engineered surfaces for functional performance,” Cirp Ann-Manuf. Techn., Vol. 57, No. 2, pp. 750-769, 2008.

2. Etsion, I., Kligerman, Y. and Halperin, G., "Analytical and experimental investigation of laser-textured mechanical seal faces," Tribology Trans., Vol. 42, No. 3, pp. 511-516, 1999.

3. Wang, Q. and Zhu, D., "Virtual texturing: Modeling the performance of lubricated contacts of engineered surfaces," J. Tribol-T Asme, Vol. 127, No. 4, pp. 722-728, 2005.

4. Kim, D. E., Cha, K. H. and Sung, I. H., "Design of surface micro-structures for friction control in micro-systems applications," Cirp Ann-Manuf. Techn., Vol. 51, No. 1, pp. 495-498, 2002.

5. Costa, H. L. and Hutchings, I. M., "Hydrodynamic lubrication of textured steel surfaces under reciprocating sliding conditions," Tribol. Int., Vol. 40, No. 8, pp. 1227-1238, 2007.

6. Zhu, D., Qu, N. S., Li, H. S., Zeng, Y. B., Li, D. L. and Qian, S. Q., "Electrochemical micromachining of microstructures of micro hole and dimple array," Cirp Ann-Manuf. Techn., Vol. 58, No. 1, pp. 177-180, 2009.

7. Wakuda, M., Yamauchi, Y., Kanzaki, S. and Yasuda, Y., "Effect of surface texturing on friction reduction between ceramic and steel materials under lubricated sliding contact," Wear, Vol. 254, No. 3-4, pp. 356-363, 2003.

8. Etsion, I., "State of the art in laser surface texturing," J. Tribol-T Asme, Vol. 127, No. 1, pp. 248-253, 2005.

9. Yi, W. and Dang-Sheng, X., "The effect of laser surface texturing on frictional performance of face seal," J. Mater. Process Tech., Vol. 197, No. 1-3, pp. 96-100, 2008.

10. Kovalchenko, A., Ajayi, O., Erdemir, A., Fenske, G. and Etsion, I., "The effect of laser surface texturing on transitions in lubrication regimes during unidirectional sliding contact," Tribol. Int., Vol. 38, No. 3, pp. 219-225, 2005.

11. Etsion, I. and Halperin, G., "A laser surface textured hydrostatic mechanical Seal," Tribology Trans., Vol. 45, No. 3, pp. 430-434, 2002.

12. Brizmer, V., Kligerman, Y. and Etsion, I., "A laser surface textured parallel thrust bearing," Tribology Trans., Vol. 46, No. 3, pp. 397-403, 2003.

13. Wang, X., Kato, K. and Adachi, K., "Running-in effect on the load-carrying capacity of a water-lubricated SiC thrust bearing," Proceedings of the Institution of Mechanical Engineers, Part J: J. Eng. Tribol., Vol. 219, No. 2, pp. 117-124, 2005.

14. Kirchner, V., Cagnon, L., Schuster, R. and Ertl, G., "Electrochemical machining of stainless steel microelements with ultrashort voltage pulses," Appl. Phys. Lett., Vol. 79, No. 11, pp. 1721-1723, 2001.

15. Schuster, R., Kirchner, V., Allongue, P. and Ertl, G., "Electrochemical micromachining," Science, Vol. 289, No. 5476, pp. 98-101, 2000.

16. Park, M. S. and Chu, C. N., "Micro-electrochemical Machining Using Multiple Tool Electrodes," J. Micromech. Microeng., Vol. 17, No. 8, pp. 1451-1457, 2007.

17. Shin, H. S., Kim, B. H. and Chu, C. N., "Analysis of the side gap resulting from micro electrochemical machining with a tungsten wire and ultrashort voltage pulses," J. Micromech. Microeng., Vol. 18, No. 7, 075009, 2008.

18. Kim, B. H., Ryu, S. H., Choi, D. K. and Chu, C. N., "Micro Electrochemical Milling," J. Micromech. Microeng., Vol. 15, No. 1, pp. 124-129, 2005.

19. Yang, I., Park, M. S. and Chu, C. N., "Micro ECM with Ultrasonic Vibrations Using a Semi-cylindrical Tool," Int. J. Precis. Eng. Manuf., Vol. 10, No. 2, pp. 5-10, 2009.

20. Kim, B. H., Na, C. W., Lee, Y. S., Choi, D. K. and Chu, C. N., "Micro electrochemical machining of 3D micro structure using dilute sulfuric acid," Cirp Ann-Manuf. Techn., Vol. 54, No. 1, pp. 191-194, 2005.

21. Wang, X., Kato, K., Adachi, K. and Aizawa, K., "Loads carrying capacity map for the surface texture design of SiC thrust bearing sliding in water," Tribol. Int., Vol. 36, No. 3, pp. 189-197, 2003.

22. Wang, X. and Kato, K., "Improving the anti-seizure ability of SiC seal in water with RIE texturing," Tribol. Lett., Vol. 14, No. 4, pp. 275-280, 2003.